



**HAL**  
open science

## **Transcripts of ceruloplasmin but not hepcidin, both major iron metabolism genes, exhibit a decreasing pattern along portocentral axis of mouse liver**

Marie-Bérengère Troadec, Alain Fautrel, Bernard Drénou, Patricia Leroyer, Emilie Camberlein, Bruno Turlin, André Guillouzo, Pierre Brissot, Olivier Loréal

### ► To cite this version:

Marie-Bérengère Troadec, Alain Fautrel, Bernard Drénou, Patricia Leroyer, Emilie Camberlein, et al.. Transcripts of ceruloplasmin but not hepcidin, both major iron metabolism genes, exhibit a decreasing pattern along portocentral axis of mouse liver. *Biochimica et Biophysica Acta - Molecular Basis of Disease*, 2008, 1782 (4), pp.239. 10.1016/j.bbadis.2007.12.009 . hal-00501561

**HAL Id: hal-00501561**

**<https://hal.science/hal-00501561>**

Submitted on 12 Jul 2010

**HAL** is a multi-disciplinary open access archive for the deposit and dissemination of scientific research documents, whether they are published or not. The documents may come from teaching and research institutions in France or abroad, or from public or private research centers.

L'archive ouverte pluridisciplinaire **HAL**, est destinée au dépôt et à la diffusion de documents scientifiques de niveau recherche, publiés ou non, émanant des établissements d'enseignement et de recherche français ou étrangers, des laboratoires publics ou privés.

## Accepted Manuscript

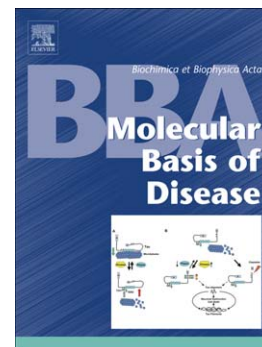
Transcripts of ceruloplasmin but not hepcidin, both major iron metabolism genes, exhibit a decreasing pattern along portocentral axis of mouse liver

Marie-Bérengère Troadec, Alain Fautrel, Bernard Drénou, Patricia Leroyer, Emilie Camberlein, Bruno Turlin, André Guillouzo, Pierre Brissot, Olivier Loréal

PII: S0925-4439(07)00239-6  
DOI: doi: [10.1016/j.bbadis.2007.12.009](https://doi.org/10.1016/j.bbadis.2007.12.009)  
Reference: BBADIS 62776

To appear in: *BBA - Molecular Basis of Disease*

Received date: 24 July 2007  
Revised date: 23 November 2007  
Accepted date: 18 December 2007



Please cite this article as: Marie-Bérengère Troadec, Alain Fautrel, Bernard Drénou, Patricia Leroyer, Emilie Camberlein, Bruno Turlin, André Guillouzo, Pierre Brissot, Olivier Loréal, Transcripts of ceruloplasmin but not hepcidin, both major iron metabolism genes, exhibit a decreasing pattern along portocentral axis of mouse liver, *BBA - Molecular Basis of Disease* (2008), doi: [10.1016/j.bbadis.2007.12.009](https://doi.org/10.1016/j.bbadis.2007.12.009)

This is a PDF file of an unedited manuscript that has been accepted for publication. As a service to our customers we are providing this early version of the manuscript. The manuscript will undergo copyediting, typesetting, and review of the resulting proof before it is published in its final form. Please note that during the production process errors may be discovered which could affect the content, and all legal disclaimers that apply to the journal pertain.

## TITLE PAGE

## Title

**TRANSCRIPTS OF CERULOPLASMIN BUT NOT HEPCIDIN, BOTH MAJOR IRON METABOLISM GENES, EXHIBIT A DECREASING PATTERN ALONG PORTOCENTRAL AXIS OF MOUSE LIVER.**

## Author Names

Marie-Bérengère Troadec <sup>1</sup>, Alain Fautrel <sup>2,3</sup>, Bernard Drénou <sup>4</sup>, Patricia Leroyer <sup>1</sup>, Emilie Camberlein <sup>1</sup>, Bruno Turlin <sup>1,3,5</sup>, André Guillouzo <sup>2</sup>, Pierre Brissot <sup>1,6</sup> and Olivier Loral <sup>1</sup>

## Affiliations

<sup>1</sup>INSERM U522 ; University of Rennes 1 ; IFR 140; <sup>2</sup>INSERM U620 ; University of Rennes 1 ; IFR 140; <sup>3</sup> IFR 140 Core HistoPathology Platform ; <sup>4</sup> Haematology Department, Mulhouse Hospital, <sup>5</sup> Department of Anatomopathology and <sup>6</sup>Liver Disease Unit, University Hospital Pontchaillou, 35033 Rennes, France.

**Short title :** iron metabolism, liver zonation and ploidy

**Keywords :** Iron metabolism; liver zonation; ploidy; ceruloplasmin; hepcidin; gene expression; laser microdissection, cytometry; mouse.

## Corresponding author

Dr Olivier LOREAL; INSERM U522, Hospital Pontchaillou, 35033 Rennes, France.  
Phone :33.2.99.54.37.37 ; Fax :33.2.99.54.01.37 e-mail : [olivier.loreal@rennes.inserm.fr](mailto:olivier.loreal@rennes.inserm.fr)

Dr Marie-Bérengère TROADEC; INSERM U522, Hospital Pontchaillou, 35033 Rennes, France. Phone :33.2.99.54.37.37 ; Fax :33.2.99.54.01.37 e-mail : [marie-berengere.troadec@univ-rennes1.fr](mailto:marie-berengere.troadec@univ-rennes1.fr)

**SUMMARY**

**Background/Aims:** During iron overload of dietary origin, iron accumulates predominantly in periportal hepatocytes. A gradient in the basal and normal transcriptional control of genes involved in iron-metabolism along the portocentral axis of liver lobules could explain this feature. Therefore, we aimed at characterizing, by quantitative RT-PCR, the expression of iron-metabolism genes in adult C57BL/6 mouse hepatocytes regarding lobular localisation, with special emphasis to cell ploidy, considering its possible relationship with lobular zonation. **Methods:** We used two methods to analyse separately periportal and perivenous liver cells: 1) a selective liver zonal destruction by digitonin prior to a classical collagenase dissociation, and 2) laser capture microdissection. We also developed a method to separate viable 4N and 8N polyploidy hepatocytes by flow cytometer. **Results:** Transcripts of ceruloplasmin, involved in iron efflux, were overexpressed in periportal areas and the result was confirmed by *in situ* hybridization study. By contrast, hepcidin 1, hemojuvelin, ferroportin, transferrin receptor 2, hfe and L-ferritin mRNAs were not differentially expressed according to either lobular zonation or polyploidisation level. **Conclusions:** At variance with glutamine or urea metabolism, iron metabolism is not featured by a metabolic zonation lying only on a basal transcriptional control. The preferential periportal expression of ceruloplasmin raises the issue of its special role in iron overload disorders involving a defect in cellular iron export.

**Abstract word count:** 216

**List of Abbreviations**

LDH: lactate dehydrogenase; SSC: Side Scatter Channel; FSC: Forward Scatter Channel; PI: Propidium Iodide; 2N: diploid cells; 4N: tetraploid cells; 8N: octoploid cells; LCM: Laser Capture Microdissection.

## INTRODUCTION

Hepatocytes are heterogeneous for metabolic functions (review in [1]) and ploidy (total cell DNA content) [2, 3] within hepatic lobules.

Periportal hepatocytes are mainly involved in ureagenesis, bile formation and glycogenesis. Perivenous (centrilobular) hepatocytes are preferentially implicated in glycolysis, lipogenesis, glutamine synthesis and xenobiotic metabolism (review in [1]). The liver metabolic zonation can be partially related to a static transcriptional zonation implicating transcriptional factors such as recently described in the Wnt/beta-catenin pathway [4], or physiological parameters including oxygen tension, blood stream, circulating factors, paracrine effects between cells or cell-cell contacts (review in [1]).

Cell ploidy is defined as the total cellular DNA content. The normal DNA content for eukaryotic cells is  $2N$  (diploid cell). Cells with more than  $2N$  chromosomes are called polyploid. DNA can be distributed in one nucleus (mononuclear) or 2 nuclei (binuclear). Hepatocytes can therefore be diploid ( $2N$ ), tetraploid ( $4N$ ) with one nucleus or tetraploid with 2 diploid nuclei, octaploid ( $8N$ ). Furthermore, the liver exhibits a peculiar distribution of hepatocyte ploidy within the lobules, and expresses biological differences between diploid and polyploid hepatocytes [5, 6]. Previous results suggested, by indirect evaluations [5, 6], a particular distribution of hepatocyte ploidy within the lobules. Indeed, diploid-enriched fractions and polyploid cells showed phenotypic markers from periportal areas and perivenous areas respectively [5].

During certain human iron overload diseases, such as HFE haemochromatosis, iron accumulates in hepatocytes following a portocentral decreasing gradient [7]. This heterogeneous distribution of iron is also observed in iron overload models of : i) genetic

origin, such in mice knock-out for *Hfe* gene (*Hfe*<sup>-/-</sup>) [8], ii) or iron-rich diet origin, such as carbonyl-iron supplemented mice [9]. Periportal hepatocytes are the first cells to receive both transferrin and non-transferrin bound iron [10] from blood flow and are therefore iron-overloaded prior to centrilobular hepatocytes. However, unexpectedly, mice knock-out for the hepcidin gene (*hepc1*<sup>-/-</sup>) mice show a perivenous iron accumulation [11] suggesting that other types of control could be implicated in addition to the blood flow.

In this study, we addressed the question of an iron metabolism zonation lying on a static mRNA expression level, on the model of glutamine or urea metabolism [4].

Distribution of iron-metabolism gene expression within liver lobules is partial, and mainly documented in rats [12, 13],. However, except for *hepcidin* and *hemojuvelin* [14] no data on the distribution of most major iron-metabolism genes is yet available in mouse, despite its recognition as a model for studying the pathophysiology of iron metabolism.

**Our aim** was to characterize the hepatic expression of iron-metabolism genes in adult mouse regarding: i) hepatocyte localisation within the liver lobules and ii) hepatocyte ploidy status. We focused our study on genes implicated in: i) the local or systemic control of iron homeostasis such as hepcidin 1 (*Hepc1* also named *Hamp1*) [15, 16], *Hfe* [17], *hemojuvelin* (*Hjv*) [18] and transferrin receptor 2 (*Tfr2*) [19, 20], ii) iron uptake : transferrin receptor 1 (*Tfr1*) [21], iii) iron storage : L-ferritin [22, 23], and iv) iron efflux : ferroportin [24-26], and ceruloplasmin [27]. Periportal and perivenous hepatocytes were separated either by selective areas destruction by digitonin prior to liver dissociation or by laser capture microdissection. Moreover, in order to isolate viable hepatocytes on the basis of DNA content, we developed a on flow cytometric method allowing further mRNA level quantification.

We found that ceruloplasmin showed a decreasing portocentral transcriptional gradient along the lobules. By contrast, no mRNA level gradient was found according to hepatocyte ploidy or along the portocentral axis of liver lobules for other iron-related genes, including hepcidin 1, hfe, hemojuvelin, transferrin receptor 2, L-ferritin and ferroportin. Our results suggest that the zonal iron accumulation observed during hepatic iron overload cannot be explained by a major static zonation of iron-metabolism transcriptional regulation in C57BL/6 mice, and suggest to take into account the role of the periportal expression of ceruloplasmin in iron overload conditions involving a defect in cellular iron efflux.

## MATERIALS AND METHODS

### Animals

Adult 20-week old C57BL/6 male mice from CERJ (Le Genest St Isle, France) were used. They were maintained under standard conditions of temperature, atmosphere and light, and experimental procedures were performed in agreement with French law and regulations (Agreement B-35-238-10). They had free access to tap water and standard AO3 diet (UAR, France).

### Selective isolation of perivenous and periportal hepatocytes by digitonin-collagenase perfusion

After anaesthesia, perivenous and periportal hepatocytes were prepared by the digitonin-collagenase perfusion method [28, 29] adapted to mouse. Hepatic veins were first ligatured. To obtain perivenous hepatocytes, the liver was first washed 3 min (10 mL/min) in HEPES buffer and then short-term perfused with 7 mM digitonin for a few seconds at 2.5 mL/min through the portal vein. The liver was then washed by an anterograde wash flow 10 min (10 mL/min) in calcium-free HEPES buffer through the inferior vena cava, followed by 8 min (10 mL/min) of enzymatic dissociation in HEPES buffer (0.025% collagenase, 0.075% CaCl<sub>2</sub>). To obtain periportal hepatocytes, destruction of perivenous areas was achieved by perfusion through the inferior vena cava and dissociation through the portal vein. Cells were then filtrated on nylon 60 $\mu$  with Leibowitz medium (Invitrogen) and settled 20 min in order to enrich the pellet in hepatocytes. Cells were washed twice in HEPES (700 rpm, 1min) and once in MEM:M119 (3v:1v; Invitrogen) in order to eliminate dead cells, and thereafter immediately frozen at -80°C until RNA extraction.

**Selective isolation of perivenous and periportal hepatic cells by Laser Capture****Microscopy (LCM)**

After anaesthesia, livers were removed, frozen in isopentane then liquid nitrogen, and stored at  $-80^{\circ}\text{C}$ . Ten  $\mu\text{m}$  thick frozen sections were cut on a cryostat (Leica, Milton Keynes, UK), mounted onto uncoated glass slides, fixed at  $-20^{\circ}\text{C}$  in 70% ethanol for 1 min, then stained with histogene (Arcturus Engineering, Mountain View, California, USA) for 5s at room temperature, washed briefly in 70% ethanol and sequentially dehydrated in 100% ethanol and xylene. The sections were then microdissected using a Veritas Laser Capture Microdissection system (LCM) (Arcturus). The settings of the InfraRed laser were: spot diameter 20  $\mu\text{m}$ , pulse duration 3500 ms and power 90 mW. On the same section, 1  $\text{mm}^2$  of perivenous and centrilobular areas were microdissected with a separated "cap". All areas were selected and collected in less than 30 min after the slide preparation. RNA isolation was performed using the PicoPure RNA isolated kit (Arcturus). RNAs were quality-checked (Ribosomal Integrated Number (Agilent) at 7.5).

**In situ Hybridization**

***Digoxigenin-labeled riboprobe preparation.*** Two-hundred/Four-hundred base pairs length gene fragment of mouse ceruloplasmin and ferroportin were cloned into pGEM-T or pGEM-Teasy vectors (Promega, Madison, WI) with T7 and SP6 promoters flanking either side. Sequence and orientation were confirmed by DNA sequencing. For each gene, both antisense and sense probes were synthesized with 1 $\mu\text{g}$  of linearized template by in vitro transcription using DIG-RNA labelling kit (Roche) following the manufacturer's instruction. The probes were ethanol precipitated and dissolved in 100  $\mu\text{L}$  of hybridization buffer (50% formamide; 5 x standard saline citrate [SSC], pH 4.5; 50  $\mu\text{g}/\text{mL}$  yeast tRNA; 1% sodium dodecyl sulfate [SDS]; and 50  $\mu\text{g}/\text{mL}$  heparin). The probes were stored at  $-80^{\circ}\text{C}$  until use.

**Tissue preparation.** Liver sections were prepared as for laser microdissection described above.

**Hybridization.** The slides were dried on a hot plate 5 min at 35°C prior to fixation in paraformaldehyde 4% in PBS at 4°C for 10min followed by 3 washes in PBS for 3 minutes each. Antisense or sense RNA probe was diluted to a final concentration of 1 ng/μL in hybridization buffer, and incubated with the tissue in a humidified chamber at 70°C for 18 hours. Free probes were removed by a sequential washing: 3 times in SSC 1x, 50% formamide, 0.1% Tween 20 for 30 min at 65°C and 2 times 30 min in 100mM maleic acid pH 7.5, 150mM NaCl, 0.1% Tween 20 (MABT) at room temperature. The tissue was then incubated in the blocking solution (MABT + 2% blocking reagent (Roche) + 20% inactivated goat serum) 1 hour at room temperature. The hybridized RNA probes were detected by anti-digoxigenin alkaline phosphatase (1:2500 dilution; Roche) in alkaline-phosphatase staining buffer (NTMT (100mM NaCl, 50mM MgCl, 100mM Tris pH9.5, 0.1%Tween20 + NBT (Promega) and BCIP (Promega)).

### **Cell ploidy**

One million freshly isolated hepatocytes were gently permeabilized in PBS 0.5% saponin, treated by 100μg/mL RNase and stained with 10μg/mL propidium iodide. DNA content analysis was performed on FACS Calibur cytometer (BD Biosciences) on the linear scaled FL2-A. Ten thousand events were recorded by Cell Quest software (BD Biosciences), and ploidy was calculated using Modfit 2.0 software (Verity Software House), after removing of doublets on FL2-A *versus* FL2-W dot plots. Mouse lymphocytes were used as control for diploidy.

**Isolation of 4N- and 8N-enriched hepatocytes by flow cytometer**

Freshly isolated hepatocytes were analyzed on FACS Calibur cytometer (BD Biosciences) equipped with a catcher tube. Linear scaled SSC-H *versus* FSC-H dot plots were used to define gates of the sort at low speed, in exclusion mode. Samples were collected, immediately concentrated, and used for viability count, ploidy verification, cell culture, or RNA extraction.

**Viability assay**

Viability of sorted hepatocytes was assayed with 0.05% trypan-blue exclusion immediately after cell sort, and by lactate dehydrogenase (LDH) release assay (LDH assay, Roche) on cell culture [30] 24h post-seeding.

**RNA extraction and quantitative real-time RT-PCR**

Total RNAs (except for LCM samples) were extracted using SV total RNA isolation system (Promega) according to manufacturer's instructions. Quality and quantity of total RNA were assayed on a lab chip device (Agilent 2100 Bioanalyser) or Nanodrop (Agilent). Two micrograms of total RNAs were reverse-transcribed using random primers and MMLV Reverse Transcriptase (Promega). Quantitative PCR was performed using qPCR MasterMix Plus for SYBR green (Eurogentec, Seraing, Belgium) on ABI prism 7000 SDS (PE-Biosystems): 95°C for 10 min and 40 cycles of 95°C for 15 seconds and 60°C for 1 min. Each amplification was duplicated. We verified genomic DNA contamination by negative control of reverse transcription and amplification efficiency by standard curves. Each result was normalized with beta-actin endogenous value. Primers are presented in Table 1.

**Statistical analysis**

A p-value, from non parametric Mann Whitney or Spearman correlation tests (StatView software), lower than 0.05 was considered as statistically significant.

ACCEPTED MANUSCRIPT

## RESULTS

### Efficiency of differential zonal liver perfusion.

Selective destruction of periportal or perivenous areas of liver lobules by digitonin (Figure 1, panels A, B and C) prior to tissue dissociation showed a classical reticular aspect of liver as described in rat [29] and mouse livers [31]. The pellets consisted mainly of hepatocytes and about  $20 \times 10^6$  hepatocytes were collected per liver with cell viability above 80%. The selectivity of liver destruction was evaluated by quantitative RT-PCR of intracellular transcriptional level of *Pepck* (phosphoenolpyruvate carboxykinase) involved in glycogenesis, known as a periportal mRNA marker [32, 33], and of *Glutamine synthetase (Gs)* (glutamine synthesis) [33, 34] and *Cyp2e1* (xenobiotic metabolism), as centrilobular mRNA markers [33-36] (Figure 2). *Pepck* mRNAs were found to be mainly expressed in periportal areas ( $p < 0.05$ ), whereas both *Gs* and *Cyp2e1* mRNAs were mainly expressed in centrilobular areas ( $p < 0.05$ ) (Figure 2A), validating the method.

### Efficiency of laser capture microdissection.

Laser Capture Microdissection (LCM) was selected as a complementary approach allowing to study various hepatic cell types, and not only hepatocytes. The histogen staining and histological architecture allowed us to easily identify portal space and centrilobular vein (Figure 3, panels A and D) with high confidence. No contamination between periportal and perivenous areas (Figure 3, panels B and C) was observed while capturing the samples. As expected (Figure 4A), we retrieved the upregulation of *Pepck* in periportal areas ( $p < 0.05$ ) whereas *Gs* and *Cyp2e1* mRNAs were predominant in perivenous areas ( $p < 0.05$ ). We noticed that the amplitude of the mRNA level was higher with LCM than with the digitonin method.

**Ceruloplasmin is overexpressed in periportal area according to the digitonin method.**

We studied hepatic mRNA expression levels of 8 genes involved in iron metabolism in periportal or perivenous hepatocytes. Results are shown in Figure 2B. *Ceruloplasmin* mRNA levels were higher in periportal areas ( $p < 0.05$ ) compared to total-liver hepatocytes. Furthermore, we also found that *Tfr2* mRNA was overexpressed in periportal and perivenous ( $p < 0.05$ ) cells compared to total-liver hepatocytes. No significant zonation was observed for mRNA levels of *Hepc1*, *Hjv*, *Ferroportin*, *Hfe*, *Tfr1*, or *L-Ferritin*.

**Ceruloplasmin and Tfr1 are overexpressed in periportal areas according to LCM.**

We found that *Ceruloplasmin* and *Tfr1* mRNA levels were higher in periportal areas than in total liver ( $p < 0.05$ ) and versus perivenous areas ( $p < 0.05$ ) (Figure 4B). This double significance confirmed the results. *Hepc1*, *Hjv*, *ferroportin*, *Hfe*, *Tfr2*, and *L-ferritin* mRNAs were equally expressed along the portocentral axis of the lobules.

**Ceruloplasmin is overexpressed in periportal areas according to *in situ* hybridization.**

In order to confirm results obtained by LCM, we performed *in situ* hybridization of ceruloplasmin and ferroportin mRNA with both antisense and sense probes (Figure 5, panels A and B, respectively). Ceruloplasmin expression was observed only in hepatocytes. No detectable signal was observed using the ceruloplasmin sense probe (negative probe). The ceruloplasmin staining was stronger in periportal hepatocytes (Figure 5A). The expression of ferroportin was not uniform but did however not present any clear gradient. Ferroportin staining was weakly detected in hepatocytes and better detected in sinusoidal cells, i.e Kupffer cells (Figure 5B). No staining was detected with the ferroportin sense probe (negative probe).

These results are in agreement with our quantitative RT-PCR findings on LCM samples. Furthermore, they confirmed the major implication of other hepatic cell types than hepatocytes, namely Kupffer cells, of the ferroportin.

### **Relationship between hepatocyte ploidy and location within the lobule.**

In this study, we isolated hepatocytes from periportal and perivenous areas by the digitonin-collagenase protocol, and we directly measured cellular DNA content in these cells by flow cytometry using propidium iodide staining (Table 2). As expected in adult mice, close to 97% of hepatocytes were polyploid (ie  $>2N$ ) [30, 37-39] (Table 2). We identified a depletion in diploid cells in the centrilobular hepatocyte subpopulation (2.9%) compared to periportal cells (6.6%) ( $p < 0.001$ ), and an enrichment in diploid hepatocytes in periportal areas ( $p < 0.01$ ) compared to controls, demonstrating that diploid hepatocytes were preferentially located around the portal triad. Interestingly, we also demonstrated that the different populations of polyploid (ie 4N, 8N) hepatocytes were homogeneously distributed within the lobule.

### **Efficient enrichment of hepatocyte ploidy sort.**

In order to isolate viable hepatocytes on the basis of DNA content, we developed a protocol to sort, by flow cytometry, fresh polyploid hepatocytes from adult mouse hepatocytes on SSC-H (granularity/cytoplasmic complexity) *versus* FSC-H (size) parameters on linear scales without using dye (Figure 5A). Sorted subpopulations were homogeneous in ploidy (Figure 5B), size, and granularity (Figure 5A). Enrichment of the 4N subpopulation was up to 96.8%, and 72.7% for the 8N hepatocytes (Figure 5C). Because diploid cells represented less than 4% of total hepatocytes, they were not sorted from adult mice liver. Moreover, propidium iodide staining of these subpopulations revealed heterogeneous populations in terms of nuclearity, with mono- and bi-nucleated cells (Figure 5D). Immediately after the sorting, as well as 24h

after seeding, viability was slightly higher in sorted subpopulations than in non-sorted whole population maintained under the same conditions, as evaluated by trypan-blue dye exclusion and by LDH release respectively (Table 3). High quality total RNA was obtained with a 28S/18S ratio of more than 1.7 as measured on a lab chip Agilent device. Moreover, cells were kept in culture up to 72h, demonstrating the viability and sterility of this protocol (data not shown).

### **Gene expression and hepatocyte ploidy.**

We assayed transcriptional levels of periportal (*Pepck*) and centrilobular (*Gs* and *Cyp2e1*) markers in 4N- and 8N-hepatocytes (Figure 6A). *Pepck* was uniformly expressed in 4N-enriched subpopulation, 8N-enriched subpopulation and total hepatocyte population. *Gs* mRNAs were overexpressed in 4N-enriched versus 8N-enriched and total-liver hepatocyte populations ( $p < 0.05$ ). *Cyp2e1* mRNAs were also overexpressed in the 4N-enriched subpopulation compared to 8N-enriched subpopulation and total hepatocyte population ( $p < 0.05$ ). In these samples, we observed a positive correlation between 18S rRNA and Beta-Actin mRNA ( $\rho = 0.676$ ,  $p < 0.05$ ) (Figure 6B) suggesting that global gene expression in hepatocytes was effectively related to DNA content unit. Previous data indicated that hepatocyte cell ploidy was correlated to nuclear RNA synthesis, RNA polymerase activity, and cellular RNA content [40, 41].

mRNA levels of genes involved in iron metabolism, *Hepc1*, *Hjv*, *ferroportin*, *Hfe*, *Tfr1*, *Tfr2* and *L-ferritin*, did not vary significantly between 4N-enriched, 8N-enriched subpopulations and total hepatocyte population (Figure 6C). However, we only observed a trend towards a decrease in expression of *ceruloplasmin* in these polyploid cells compared to total liver hepatocytes suggesting that diploid hepatocytes are the main source of this protein.

## DISCUSSION

In this study, we addressed the question of a zonation of iron metabolism mRNA expression in basal condition which could secondarily play a role during iron overload diseases.

Periportal or centrilobular hepatic cells were collected either by specific zonation destruction with digitonin prior to liver dissociation or by laser capture microdissection (LCM). Liver dissociation and LCM allowed us to obtain gene expression results in hepatocytes only and in hepatic cells, including sinusoidal cells, respectively. Furthermore, these methods allowed us to measure mRNA levels by quantitative PCR, a more quantitative methodology than mRNA *in situ* hybridization.

As expected, overexpression of *Pepck* mRNAs [32, 33] in periportal areas and overexpression of *glutamine synthetase* [33, 34] and *Cyp2e1* [35, 36] mRNAs in centrilobular areas validated the efficiency of both methods. However, differences revealed by LCM were sharper between periportal and perivenous areas. This was well illustrated by glutamine synthetase, an hepatocyte specific gene (Figures 2 and 4). A limitation of the digitonin-dissociation methodology is that periportal, perivenous and control cells were not originating from the same animals, a potential source of increased variability. By contrast with digitonin-dissociation methodology, LCM-extracted areas contained a majority of hepatocytes but also non parenchymal cells. This feature could explain our data on mRNA level of *Tfr1*, which is overexpressed in periportal areas of adult mice using LCM method only. This suggests that non hepatocyte cell types could be involved in the portocentral decreasing gradient of *Tfr1*, in accordance with data reporting changes in Tfr1 protein expression in aging rats [42]. Indeed, Tfr1 protein staining was mainly observed within sinusoidal cells and in periportal areas in adult rats, whereas it was parenchymal and perivenous in younger rats.

Using mRNA in situ hybridization, previous data reported that *Hfe*, *Tfr2*, *Tf*, *Tfr1* and *L-ferritin* mRNAs in rat [12, 13] and *hepcidin* mRNA in mouse [14] were homogeneously expressed within the lobules in the hepatocytes. We found accordingly that, in the liver of adult C57BL/6 mouse, *hepcidin 1*, *Hfe*, *Tfr2* and *L-ferritin* mRNAs did not show a portocentrolobular gradient. However, we found that isolated hepatocytes expressed *Tfr2* with an unusual pattern corresponding to both periportal and centrilobular veins. A better understanding of the exact role of *Tfr2* gene, which is not directly implicated in hepatocyte iron uptake, in the control of *hepcidin* expression [20] and more globally in iron metabolism will help to understand such pattern.

Haemojuvelin is a major regulator of *hepcidin* expression [18] which is a negative regulator of the iron export activity of ferroportin [43]. We did not detect any zonation for either *ferroportin* or *hemojuvelin* mRNAs at variance with authors who found that the levels of *ferroportin* mRNA in the rat [12] and activity of *hemojuvelin* promoter in the mouse [14] were higher in periportal hepatocytes. We confirmed our data on *ferroportin* expression by in situ hybridization. A species-difference could be possible for *ferroportin* expression. The difference with previous published results for *hemojuvelin* could suggest : i) a strain specificity [44-46], ii) a perturbation in the *hemojuvelin* promoter activity or, iii) an alteration of the upstream-transcript stability in periportal areas in *hemojuvelin*-deficient transgenic mice [14].

Using the ploidy approach, we found that the level of *hepcidin 1*, *hemojuvelin*, *ferroportin*, *Hfe*, *Tfr1*, *Tfr2*, *ceruloplasmin* and *L-ferritin* mRNAs normalized on actin mRNA level were similar in 4N- and 8N-enriched hepatocyte subpopulations compared to total-liver hepatocytes suggesting that the transcriptional activity of these genes is correlated with cell

DNA content. Several authors have explored the relationship between ploidy and functional activity. Some have found that the rate of protein synthesis was directly proportional to the degree of cell ploidy [47-52], others have demonstrated that rat polyploid-enriched fractions showed higher cytochrome P450 [5], and glutamine synthetase [6] activities and, in contrast, that diploid hepatocytes presented a higher ceruloplasmin biosynthetic rate [5], suggesting exogenous control factors of these gene expressions, such as cell-cell contact or circulating soluble factors. Our results on *Cyp2e1*, *Gs* and *ceruloplasmin* mRNAs expression reinforce this view.

Our data, indicating about a two-fold induction of *ceruloplasmin* mRNA level in periportal areas, could be associated to the periportal increase of ceruloplasmin protein synthesis previously reported in rat [5]. We also confirmed the increase in ceruloplasmin mRNA expression in periportal hepatocytes by in situ hybridization. Ceruloplasmin is a ferroxidase, which is secreted in the plasma by the liver. Its function depends on the presence of an iron exporter, such as ferroportin, a membrane protein. The presence of extracellular ceruloplasmin is required for proper iron export. Thus, ceruloplasmin deficiency had been previously associated with the development of iron overload in mice [53] and in humans, since patients with aceruloplasminemia present iron overload, including liver iron overload [54]. Furthermore, at local level, high modulation of ceruloplasmin was reported in *Usp2* knock-out mice, exhibiting iron overload secondary to the lack of hepcidin expression found in this model [55]. Our results clearly showed that the expression patterns of ferroportin and ceruloplasmin did not merge, suggesting that secretion site of ceruloplasmin differs from its sites of action. However, we assume that the particular location of ceruloplasmin expression in periportal hepatocytes could have a direct physiological implication in adjusting the level of synthesis of Ceruloplasmin to serum iron. Ceruloplasmin could act as a tuner of iron

export, locally but also at systemic level. Moreover, the overexpression of ceruloplasmin in periportal hepatocytes could explain, at least partially, the centrilobular accumulation of iron in *hepc1* knock out mice [11] by an extra iron efflux in periportal areas at the expense of a weaker iron efflux in centrilobular areas. The role of periportal expression of ceruloplasmin in disorders related to altered hepcidin-ferroportin pathways controlling iron export requires further studies.

***In conclusion***, in this study, *ceruloplasmin* mRNA, and *Tfr1* mRNA were the only iron-metabolism genes which exhibited a decreasing mRNA level gradient along the portocentral axis of hepatic lobules. Other genes, *hepcidin 1*, *hemojuvelin*, *ferroportin*, *Hfe*, and *L-ferritin*, were not differentially expressed within liver lobules. Therefore, the hepatic iron distribution observed during genetic haemochromatosis in liver is unlikely related to a static transcriptional zonation. However, physiological implication of periportal location of ceruloplasmin may be strategic in the control of iron metabolism, and should be taken into account when considering the cell mechanisms involved in iron overload diseases characterized by altered cellular iron export.

**ACKNOWLEDGEMENTS**

The authors thank Catherine Ribaud for technical assistance with mice care at INSERM U522 (Rennes), Pascale Bellaud for technical assistance on the laser microdissection facilities of IFR140 (Rennes), Carole Gautier, Valérie Dupé and Audrey Fleury for helpful advises for in situ hybridizations. This work was supported by INSERM, a PRIR nb.139 of the Région Bretagne, the Association Fer et Foie, and the LSHM-CT-2006-037296 European Community Grant.

**REFERENCES**

- [1] K. Jungermann and T. Kietzmann, Zonation of parenchymal and nonparenchymal metabolism in liver, *Annu Rev Nutr* 16 (1996) 179-203.
- [2] R. Carriere, Polyploid cell reproduction in normal adult rat liver, *Exp Cell Res* 46 (1967) 533-40.
- [3] W.Y. Brodsky and I.V. Uryvaeva, Cell polyploidy: its relation to tissue growth and function, *Int Rev Cytol* 50 (1977) 275-332.
- [4] S. Benhamouche, T. Decaens, C. Godard, R. Chambrey, D.S. Rickman, C. Moinard, M. Vasseur-Cognet, C.J. Kuo, A. Kahn, C. Perret and S. Colnot, Apc tumor suppressor gene is the "zonation-keeper" of mouse liver, *Dev Cell* 10 (2006) 759-70.
- [5] P. Rajvanshi, D. Liu, M. Ott, S. Gagandeep, M.L. Schilsky and S. Gupta, Fractionation of rat hepatocyte subpopulations with varying metabolic potential, proliferative capacity, and retroviral gene transfer efficiency, *Exp Cell Res* 244 (1998) 405-19.
- [6] J.C. Osypiw, R.L. Allen and D. Billington, Subpopulations of rat hepatocytes separated by Percoll density-gradient centrifugation show characteristics consistent with different acinar locations, *Biochem J* 304 ( Pt 2) (1994) 617-24.
- [7] T.C. Iancu, Y. Deugnier, J.W. Halliday, L.W. Powell and P. Brissot, Ultrastructural sequences during liver iron overload in genetic hemochromatosis, *J Hepatol* 27 (1997) 628-38.
- [8] X.Y. Zhou, S. Tomatsu, R.E. Fleming, S. Parkkila, A. Waheed, J. Jiang, Y. Fei, E.M. Brunt, D.A. Ruddy, C.E. Prass, R.C. Schatzman, R. O'Neill, R.S. Britton, B.R. Bacon and W.S. Sly, HFE gene knockout produces mouse model of hereditary hemochromatosis, *Proc Natl Acad Sci U S A* 95 (1998) 2492-7.

- [9] C. Pigeon, B. Turlin, T.C. Iancu, P. Leroyer, J. Le Lan, Y. Deugnier, P. Brissot and O. Loreal, Carbonyl-iron supplementation induces hepatocyte nuclear changes in BALB/CJ male mice, *J Hepatol* 30 (1999) 926-34.
- [10] P. Brissot, T.L. Wright, W.L. Ma and R.A. Weisiger, Efficient clearance of non-transferrin-bound iron by rat liver. Implications for hepatic iron loading in iron overload states, *J Clin Invest* 76 (1985) 1463-70.
- [11] J.C. Lesbordes-Brion, L. Viatte, M. Bennoun, D.Q. Lou, G. Ramey, C. Houbron, G. Hamard, A. Kahn and S. Vaulont, Targeted disruption of the hepcidin 1 gene results in severe hemochromatosis, *Blood* 108 (2006) 1402-5.
- [12] A.S. Zhang, S. Xiong, H. Tsukamoto and C.A. Enns, Localization of iron metabolism-related mRNAs in rat liver indicate that HFE is expressed predominantly in hepatocytes, *Blood* 103 (2004) 1509-14.
- [13] K.A. Basclain and G.P. Jeffrey, Coincident increase in periportal expression of iron proteins in the iron-loaded rat liver, *J Gastroenterol Hepatol* 14 (1999) 659-68.
- [14] V. Niederkofler, R. Salie and S. Arber, Hemojuvelin is essential for dietary iron sensing, and its mutation leads to severe iron overload, *J Clin Invest* 115 (2005) 2180-6.
- [15] C. Pigeon, G. Ilyin, B. Courselaud, P. Leroyer, B. Turlin, P. Brissot and O. Loreal, A new mouse liver-specific gene, encoding a protein homologous to human antimicrobial peptide hepcidin, is overexpressed during iron overload, *J Biol Chem* 276 (2001) 7811-9.
- [16] G. Nicolas, M. Bennoun, I. Devaux, C. Beaumont, B. Grandchamp, A. Kahn and S. Vaulont, Lack of hepcidin gene expression and severe tissue iron overload in upstream stimulatory factor 2 (USF2) knockout mice, *Proc Natl Acad Sci U S A* 98 (2001) 8780-5.

- [17] J.N. Feder, D.M. Penny, A. Irrinki, V.K. Lee, J.A. Lebron, N. Watson, Z. Tsuchihashi, E. Sigal, P.J. Bjorkman and R.C. Schatzman, The hemochromatosis gene product complexes with the transferrin receptor and lowers its affinity for ligand binding, *Proc Natl Acad Sci U S A* 95 (1998) 1472-7.
- [18] G. Papanikolaou, M.E. Samuels, E.H. Ludwig, M.L. MacDonald, P.L. Franchini, M.P. Dube, L. Andres, J. MacFarlane, N. Sakellaropoulos, M. Politou, E. Nemeth, J. Thompson, J.K. Risler, C. Zaborowska, R. Babakaiff, C.C. Radomski, T.D. Pape, O. Davidas, J. Christakis, P. Brissot, G. Lockitch, T. Ganz, M.R. Hayden and Y.P. Goldberg, Mutations in HFE2 cause iron overload in chromosome 1q-linked juvenile hemochromatosis, *Nat Genet* 36 (2004) 77-82.
- [19] H. Kawabata, R. Yang, T. Hirma, P.T. Vuong, S. Kawano, A.F. Gombart and H.P. Koeffler, Molecular cloning of Transferrin Receptor 2. A new member of the transferrin receptor-like family, *J Biol Chem* 274 (1999) 20826-20832.
- [20] E. Nemeth, A. Roetto, G. Garozzo, T. Ganz and C. Camaschella, Heparin is decreased in TFR2 hemochromatosis, *Blood* 105 (2005) 1803-6.
- [21] P.A. Seligman, R.B. Schleicher and R.H. Allen, Isolation and characterization of the transferrin receptor from human placenta, *J Biol Chem* 254 (1979) 9943-6.
- [22] G.C. Ford, P.M. Harrison, D.W. Rice, J.M. Smith, A. Treffry, J.L. White and J. Yariv, Ferritin: design and formation of an iron-storage molecule, *Philos Trans R Soc Lond B Biol Sci* 304 (1984) 551-65.
- [23] S. Levi, S.J. Yewdall, P.M. Harrison, P. Santambrogio, A. Cozzi, E. Rovida, A. Albertini and P. Arosio, Evidence of H- and L-chains have co-operative roles in the iron-uptake mechanism of human ferritin, *Biochem J* 288 (1992) 591-6.
- [24] A.T. McKie, P. Marciani, A. Rolfs, K. Brennan, K. Wehr, D. Barrow, S. Miret, A. Bomford, T.J. Peters, F. Farzaneh, M.A. Hediger, M.W. Hentze and R.J. Simpson, A

- novel duodenal iron-regulated transporter, IREG1, implicated in the basolateral transfer of iron to the circulation, *Molecular Cell* 5 (2000) 299-309.
- [25] A. Donovan, A. Brownlie, Y. Zhou, J. Shepard, S.J. Pratt, J. Moynihan, B.H. Paw, A. Drejer, B. Barut, A. Zapata, T.C. Law, C. Brugnara, S.E. Lux, G.S. Pinkus, J.L. Pinkus, P.D. Kingsley, J. Palis, M.D. Fleming, N.C. Andrews and L.I. Zon, Positional cloning of zebrafish ferroportin1 identifies a conserved vertebrate iron exporter, *Nature* 403 (2000) 776-81.
- [26] S. Abboud and D.J. Haile, A novel mammalian iron-regulated protein involved in intracellular iron metabolism, *J Biol Chem* 275 (2000) 19906-12.
- [27] C.K. Mukhopadhyay, Z.K. Attieh and P.L. Fox, Role of ceruloplasmin in cellular iron uptake, *Science* 279 (1998) 714-7.
- [28] K.O. Lindros and K.E. Penttila, Digitonin-collagenase perfusion for efficient separation of periportal or perivenous hepatocytes, *Biochem J* 228 (1985) 757-60.
- [29] E. Wodey, A. Fautrel, M. Rissel, M. Tanguy, A. Guillouzo and Y. Malledant, Halothane-induced cytotoxicity to rat centrilobular hepatocytes in primary culture is not increased under low oxygen concentration, *Anesthesiology* 79 (1993) 1296-303.
- [30] M.B. Troadec, B. Courselaud, L. Detivaud, C. Haziza-Pigeon, P. Leroyer, P. Brissot and O. Loreal, Iron overload promotes Cyclin D1 expression and alters cell cycle in mouse hepatocytes, *J Hepatol* 44 (2006) 391-9.
- [31] H. Taniai, I.N. Hines, S. Bharwani, R.E. Maloney, Y. Nimura, B. Gao, S.C. Flores, J.M. McCord, M.B. Grisham and T.Y. Aw, Susceptibility of murine periportal hepatocytes to hypoxia-reoxygenation: role for NO and Kupffer cell-derived oxidants, *Hepatology* 39 (2004) 1544-52.

- [32] J.M. Ruijter, R.G. Gieling, M.M. Markman, J. Hagoort and W.H. Lamers, Stereological measurement of porto-central gradients in gene expression in mouse liver, *Hepatology* 39 (2004) 343-52.
- [33] V.M. Christoffels, H. Sassi, J.M. Ruijter, A.F. Moorman, T. Grange and W.H. Lamers, A mechanistic model for the development and maintenance of portocentral gradients in gene expression in the liver, *Hepatology* 29 (1999) 1180-92.
- [34] A. Cadoret, C. Ovejero, B. Terris, E. Souil, L. Levy, W.H. Lamers, J. Kitajewski, A. Kahn and C. Perret, New targets of beta-catenin signaling in the liver are involved in the glutamine metabolism, *Oncogene* 21 (2002) 8293-301.
- [35] G.T. Wagenaar, R.A. Chamuleau, J.G. de Haan, M.A. Maas, P.A. de Boer, F. Marx, A.F. Moorman, W.M. Frederiks and W.H. Lamers, Experimental evidence that the physiological position of the liver within the circulation is not a major determinant of zonation of gene expression, *Hepatology* 18 (1993) 1144-53.
- [36] L. Chen, G.J. Davis, D.W. Crabb and L. Lumeng, Intrasplenic transplantation of isolated periportal and perivenous hepatocytes as a long-term system for study of liver-specific gene expression, *Hepatology* 19 (1994) 989-98.
- [37] P.O. Seglen, DNA ploidy and autophagic protein degradation as determinants of hepatocellular growth and survival, *Cell Biol Toxicol* 13 (1997) 301-15.
- [38] J.C. Garrison, T.U. Bisel, P. Peterson and E.M. Uyeki, Changes in hepatocyte ploidy in response to chromium, analyzed by computer-assisted microscopy, *Fundam Appl Toxicol* 14 (1990) 346-55.
- [39] S. Madra, J. Styles and A.G. Smith, Perturbation of hepatocyte nuclear populations induced by iron and polychlorinated biphenyls in C57BL/10ScSn mice during carcinogenesis, *Carcinogenesis* 16 (1995) 719-27.

- [40] I.R. Johnston, A.P. Mathias, F. Pennington and D. Ridge, Distribution of RNA polymerase activity among the various classes of liver nuclei, *Nature* 220 (1968) 668-72.
- [41] P.O. Seglen, Protein-catabolic stage of isolated rat hepatocytes, *Biochim Biophys Acta* 496 (1977) 182-91.
- [42] R. Sciot, G. Verhoeven, P. Van Eyken, J. Cailleau and V.J. Desmet, Transferrin receptor expression in rat liver: immunohistochemical and biochemical analysis of the effect of age and iron storage, *Hepatology* 11 (1990) 416-27.
- [43] E. Nemeth, M.S. Tuttle, J. Powelson, M.B. Vaughn, A. Donovan, D.M. Ward, T. Ganz and J. Kaplan, Heparin regulates cellular iron efflux by binding to ferroportin and inducing its internalization, *Science* 306 (2004) 2090-3.
- [44] R.C. Leboeuf, D. Tolson and J.W. Heinecke, Dissociation between tissue iron concentrations and transferrin saturation among inbred mouse strains, *J Lab Clin Med* 126 (1995) 128-36 issn: 0022-2143.
- [45] M. Bensaid, S. Fruchon, C. Mazeres, S. Bahram, M.P. Roth and H. Coppin, Multigenic control of hepatic iron loading in a murine model of hemochromatosis, *Gastroenterology* 126 (2004) 1400-8.
- [46] B. Courselaud, M.B. Troadec, S. Fruchon, G. Ilyin, N. Borot, P. Leroyer, H. Coppin, P. Brissot, M.P. Roth and O. Loreal, Strain and gender modulate hepatic hepcidin 1 and 2 mRNA expression in mice, *Blood Cells Mol Dis* 32 (2004) 283-9.
- [47] N.C. Martin, C.T. McCullough, P.G. Bush, L. Sharp, A.C. Hall and D.J. Harrison, Functional analysis of mouse hepatocytes differing in DNA content: volume, receptor expression, and effect of IFN $\gamma$ , *J Cell Physiol* 191 (2002) 138-44.

- [48] E. Le Rumeur, C. Beaumont, C. Guillouzo, M. Rissel, M. Bourel and A. Guillouzo, All normal rat hepatocytes produce albumin at a rate related to their degree of ploidy, *Biochem Biophys Res Commun* 101 (1981) 1038-46.
- [49] A. Tulp, J. Welagen and P. Emmelot, Separation of intact rat hepatocytes and rat liver nuclei into ploidy classes by velocity sedimentation at unit gravity, *Biochim Biophys Acta* 451 (1976) 567-82.
- [50] C.J. Van Noorden, I.M. Vogels, G. Fronik and R.D. Bhattacharya, Ploidy class-dependent variations during 24 h of glucose-6-phosphate and succinate dehydrogenase activity and single-stranded RNA content in isolated rat hepatocytes, *Exp Cell Res* 155 (1984) 381-8.
- [51] C.J. Van Noorden, I.M. Vogels, J.M. Houtkooper, G. Fronik, J. Tas and J. James, Glucose-6-phosphate dehydrogenase activity in individual rat hepatocytes of different ploidy classes. I. Developments during postnatal growth, *Eur J Cell Biol* 33 (1984) 157-62.
- [52] E. Le Rumeur, C. Guguen-Guillouzo, C. Beaumont, A. Saunier and A. Guillouzo, Albumin secretion and protein synthesis by cultured diploid and tetraploid rat hepatocytes separated by elutriation, *Exp Cell Res* 147 (1983) 247-54.
- [53] Z.L. Harris, A.P. Durley, T.K. Man and J.D. Gitlin, Targeted gene disruption reveals an essential role for ceruloplasmin in cellular iron efflux, *Proc Natl Acad Sci U S A* 96 (1999) 10812-7.
- [54] N.E. Hellman, M. Schaefer, S. Gehrke, P. Stegen, W.J. Hoffman, J.D. Gitlin and W. Stremmel, Hepatic iron overload in aceruloplasminaemia, *Gut* 47 (2000) 858-60.
- [55] L. Viatte, J.C. Lesbordes-Brion, D.Q. Lou, M. Bennoun, G. Nicolas, A. Kahn, F. Canonne-Hergaux and S. Vaulont, Deregulation of proteins involved in iron metabolism in hepcidin-deficient mice, *Blood* 105 (2005) 4861-4.

**FIGURE LEGENDS****Figure 1: Selective zonal destruction in liver mouse.**

To obtain periportal or perivenous hepatocytes, mouse liver was perfused by inferior vena cava or portal vein by digitonin, prior to classical liver dissociation. (A) Destruction of selected zones showed a typical reticular aspect; white zones correspond to dead cells in periportal (B) or perivenous areas (C). Original magnification x1.5 (A) and x10 (B and C).

**Figure 2: mRNA expression levels in periportal and perivenous hepatocytes obtained by liver perfusion.**

mRNA levels were obtained by quantitative RT-PCR, and expressed as  $\log_2(\text{zones}/\text{control})$ . Controls corresponded to total-liver hepatocytes. Mean  $\pm$  SD. \* $p < 0.05$ , Mann Whitney test, between samples and control (single star), or between centrilobular and periportal cells (star with bracket). (A) mRNA levels of markers from periportal or perivenous liver zones. Pepck: phosphoenolpyruvate carboxykinase, Gs: glutamine synthetase, Cyp2e1: cytochrome P450 2e1. (B) mRNA levels of genes implicated in iron metabolism. Hcp1, hepcidin, Hjuv, hemojuvelin, Tfrc, ferroportin, Cerul, ceruloplasmin, Hfe, transferrin receptor 1, Tfrc2, transferrin receptor 2 and L-ferritin.

**Figure 3: Laser capture microdissection of liver lobules.**

Thin 10  $\mu\text{m}$  slides of liver were stained by histogen (panels A to C). (A1) Typical portal space with portal vein (pv) and hepatic artery (ha) and biliary canaliculi (bc), and centrilobular vein (cv) are well seen (original magnification x 200). From these structures, hepatocytes from both periportal and perinuous areas can be selected. (A2) Different areas were selected on the

basis of the histological features of periportal to perivenous areas and the histogen staining. We captured first the periportal areas (panels B1 and B2), then the perivenous areas (panels C1 and C2). B1 and C1 show the remaining tissue whereas B2 and C2 show the captured samples from which RNAs were extracted. Original magnification x20.

**Figure 4: mRNA expression levels in periportal and perivenous liver tissue isolated by Laser Capture Microdissection.**

mRNA levels were obtained by quantitative RT-PCR, and expressed as  $\log_2(\text{captured zones}/\text{captured total liver})$ . Mean  $\pm$  SD. \* $p < 0.05$ , Mann Whitney test, between captured areas and captured total liver (single star), or between perivenous and periportal cells (star with bracket). (A) mRNA levels of markers from periportal or perivenous liver zones. Pepck: phosphoenolpyruvate carboxykinase, Gs: glutamine synthetase, Cyp2e1: cytochrome P450 2e1. (B) mRNA levels of genes implicated in iron metabolism. Heparin (Hepc1), hemojuvelin (Hjv), ferroportin, ceruloplasmin, Hfe, transferrin receptor 1 (Tfr1), transferrin receptor 2 (Tfr2) and L-ferritin.

**Figure 5: In situ hybridization analysis of hepatic ceruloplasmin and ferroportin mRNAs expression.**

*In situ* hybridization analysis of Ceruloplasmin (panel A) and Ferroportin (panel B) in mouse liver. For each gene, the images from the analysis of both antisense (gene-specific probe) and sense probes (negative control) are shown. Incubation times for the development: ceruloplasmin: 50h ; Ferroportin: 60h. \* indicates Kupffer cells. Pv indicates portal vein, cv, centrilobular vein. Original magnification x200.

**Figure 6: Separation of adult mouse hepatocytes on size and granularity criteria.**

Viable mouse hepatocytes were sorted on (A) SSC-H (granularity/complexity) *versus* FSC-H (size) parameters on flow cytometer without using any dye, detergent or fixation. (B) An aliquot of cells was stained by propidium iodide and analysed for cell DNA content on FL2-A by Cell Quest software. (C) Distribution of ploidy was analysed by Modfit software in 18-20-week old C57BL/6 mice (n=8) and in sorted hepatocytes (n=3 each subpopulation). Mean +/- SD of percentage of total cell population. (D) Nuclearity was visualized by a propidium iodide staining and revealed an heterogeneity of 4N- and 8N-enriched subpopulations.

**Figure 7: mRNA expression levels in 4N- and 8N-enriched hepatocyte subpopulations.**

mRNA levels were obtained by quantitative RT-PCR, and expressed as  $\log_2(\text{subpopulation/control})$ . Controls correspond to total-liver hepatocytes. Mean +/- SD. \* $p < 0.05$ , Mann Whitney test between samples and control (single star), or between 4N- and 8N-enriched hepatocytes (star with bracket). (A) mRNA levels of markers from periportal or perivenous liver zones. Pepck: phosphoenolpyruvate carboxykinase, Gs: Glutamine synthetase, Cyp2e1: cytochrome p450 2E1. (B) Correlation of Cycle threshold values (Ct) of 18S rRNA and actin mRNA (n=12) \* $p < 0.05$ , Spearman test. (C) mRNA levels of genes implicated in iron metabolism. Hpcidin (Hpc1), Hemojuvelin (Hjv), Ferroportin, Ceruloplasmin, Hfe, Transferrin receptor 1 (Tfr1), Transferrin receptor 2 (Tfr2) and L-Ferritin.

Symbol	Gene name	Official gene symbol	Forward	Reverse
<i>Pepck</i>	phosphoenolpyruvate carboxykinase	<i>Pck1</i>	ccacagctgctgcagaaca	gaagggtcgcattggcaaa
<i>Cyp2e1</i>	cytochrome P450 2E1	<i>Cyp2e1</i>	tgcaagtcgagacaggatga	ggacgaggtgatgaatctctga
<i>Gs</i>	glutamine synthetase	<i>Glu1</i>	caggctgccataccaactca	tcctcaatgcactcagacat
<i>18S</i>	-		tgcaattattccccatgaacg	gcttatgacccgcactactgg
<i>Actin</i>	beta actin	<i>Actb</i>	gacggccaagtcatcactattg	ccacaggattccataccaaga
<i>Hepc1</i>	hepcidin1	<i>Hamp</i>	cctatctccatcaacagatg	aacagataccacactgggaa
<i>Hjv</i>	hemojuvelin	<i>Hfe2</i>	aagtggcattgtctggcag	gttggtgccagtctccaaaag
<i>Ferroportin</i>	ferroportin	<i>Slc40a1</i>	gctgctagaatcggtcttgg	cagcaactgtgtcaccgtcaa
<i>Ceruloplasmin</i>	ceruloplasmin	<i>Cp</i>	gggagccgtctaccctgataa	ttgtcatcagccgtgaaa
<i>Hfe</i>	Hfe	<i>Hfe</i>	gagcaagtgtgcccctccaagtct	aaggaaggctcaggaggaacc
<i>Tfr1</i>	transferrin receptor 1	<i>Tfrc</i>	tcatagggaaatcaatgatcga	gcccagaagatatgtcgaa
<i>Tfr2</i>	transferrin receptor 2	<i>Tfr2</i>	agtggcgacgttgaaca	tcaggcacctccttggc
<i>L-Ferritin</i>	L-ferritin	<i>Ftl</i>	cagtctgcaccgtctctcg	gtcatggctgatccggagtag

**Table 1: Primers used for quantitative real-time RT-PCR.**

hepatocyte location	n=	Cell ploidy (%)		
		2N	4N	8N
periportal	6	6.6 +/-1.4 (p<0.05/control)	65.0 +/-4.8 (ns)	28.4 +/-4.4 (ns)
centrilobular	8	2.9 +/-1.6 (p<0.001/periportal)	66.5 +/-5.2 (ns)	30.6 +/-4.8 (ns)
total-liver hepatocytes	2	3.0 (2.3-3.8)	58.7 (51.5-65.8)	38.3 (31.8-44.8)

**Table 2: Hepatocyte ploidy in the hepatic periportal and perivenous areas.**

Isolation of periportal or perivenous hepatocytes was performed by a selective destruction of liver areas by digitonin prior to classical liver dissociation. Cell ploidy was evaluated on propidium iodide staining of hepatocytes on flow cytometer. Mean+/- SD. Mann Whitney test. ns: non significant

Hepatocyte subpopulation	n=	Viability (%)	Cell death
			(mU LDH release/mg proteins)
4N-enriched hepatocytes	3	86.7 +/- 6.1	4266.1 +/- 902 *
8N-enriched hepatocytes	3	94.2 +/- 2.0 *	4657.4 +/- 1002 *
Total liver cell population	3	76.3 +/- 5.5	6413.1 +/- 1333

**Table 3: Viability of 4N- and 8N-enriched hepatocyte subpopulations.**

4N- and 8N-enriched subpopulations were obtained from 20-week old C57BL/6 mouse hepatocytes. Immediately after sorts, hepatocyte viability was assayed by trypan-blue exclusion. Sorted hepatocytes were plated in culture and cell death was evaluated by LDH release assay (mU/mg proteins), 24h after seeding. Mean+/-SD. \*p<0.05, Mann Whitney test.

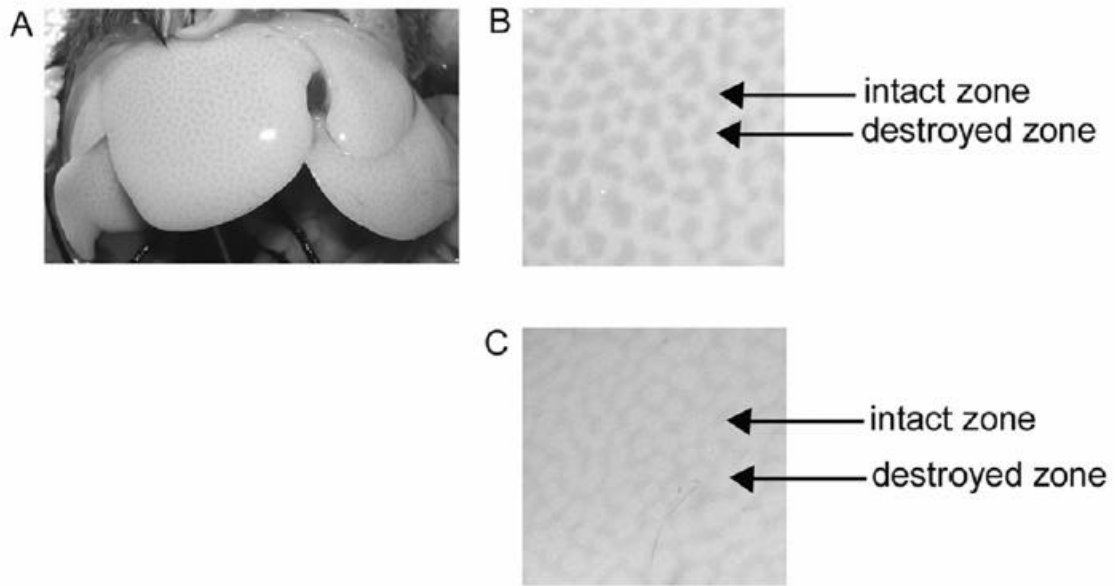


Figure 1

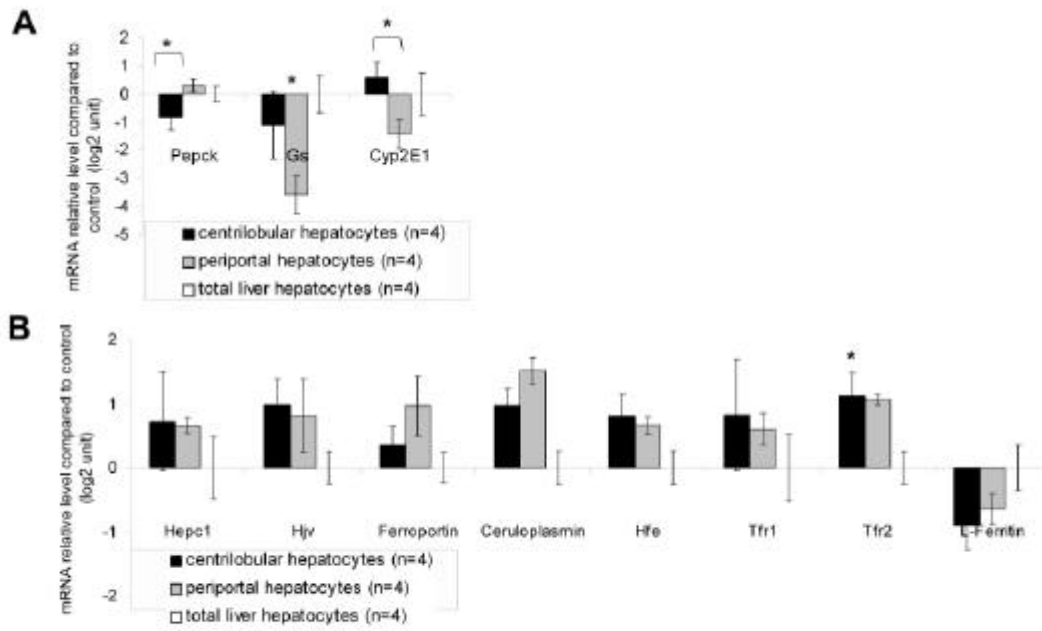


Figure 2

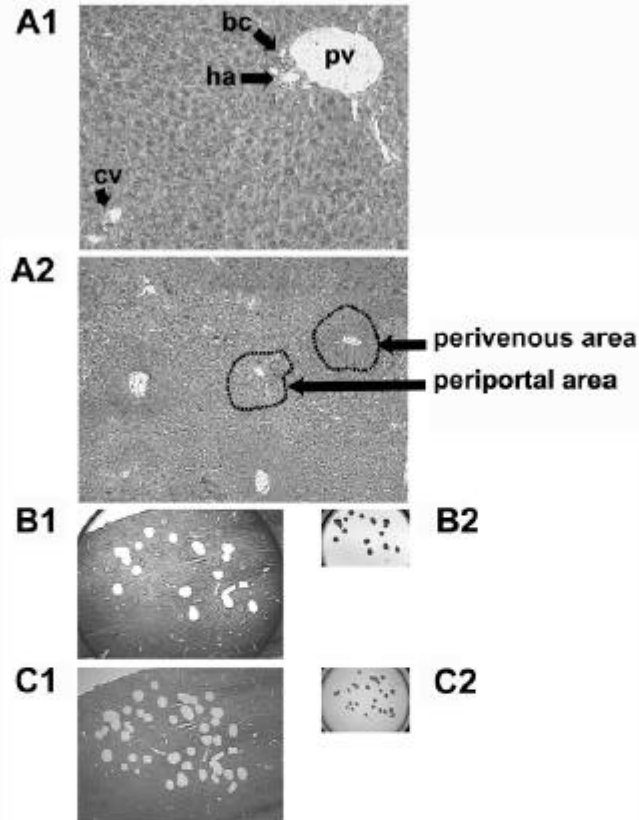


Figure 3

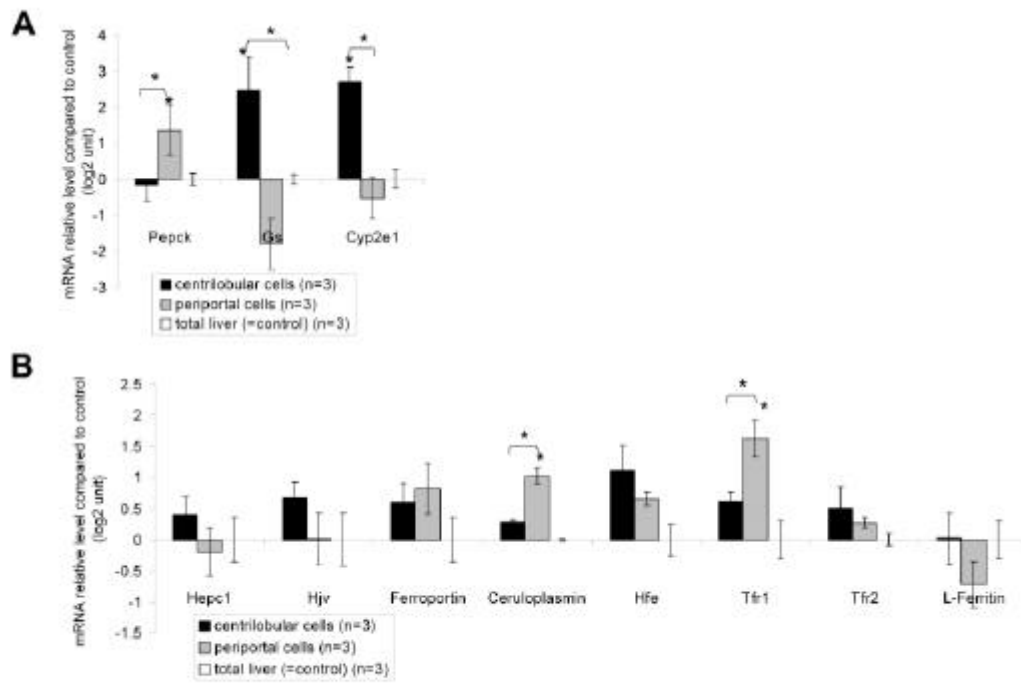


Figure 4

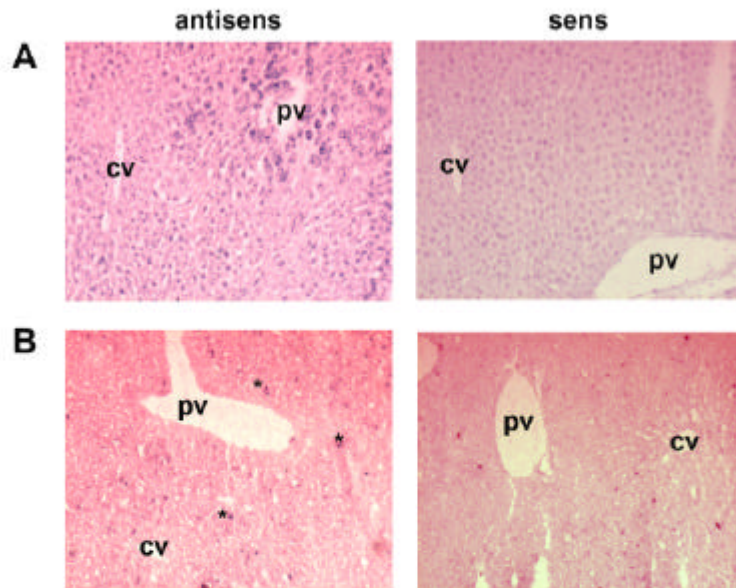


Figure 5

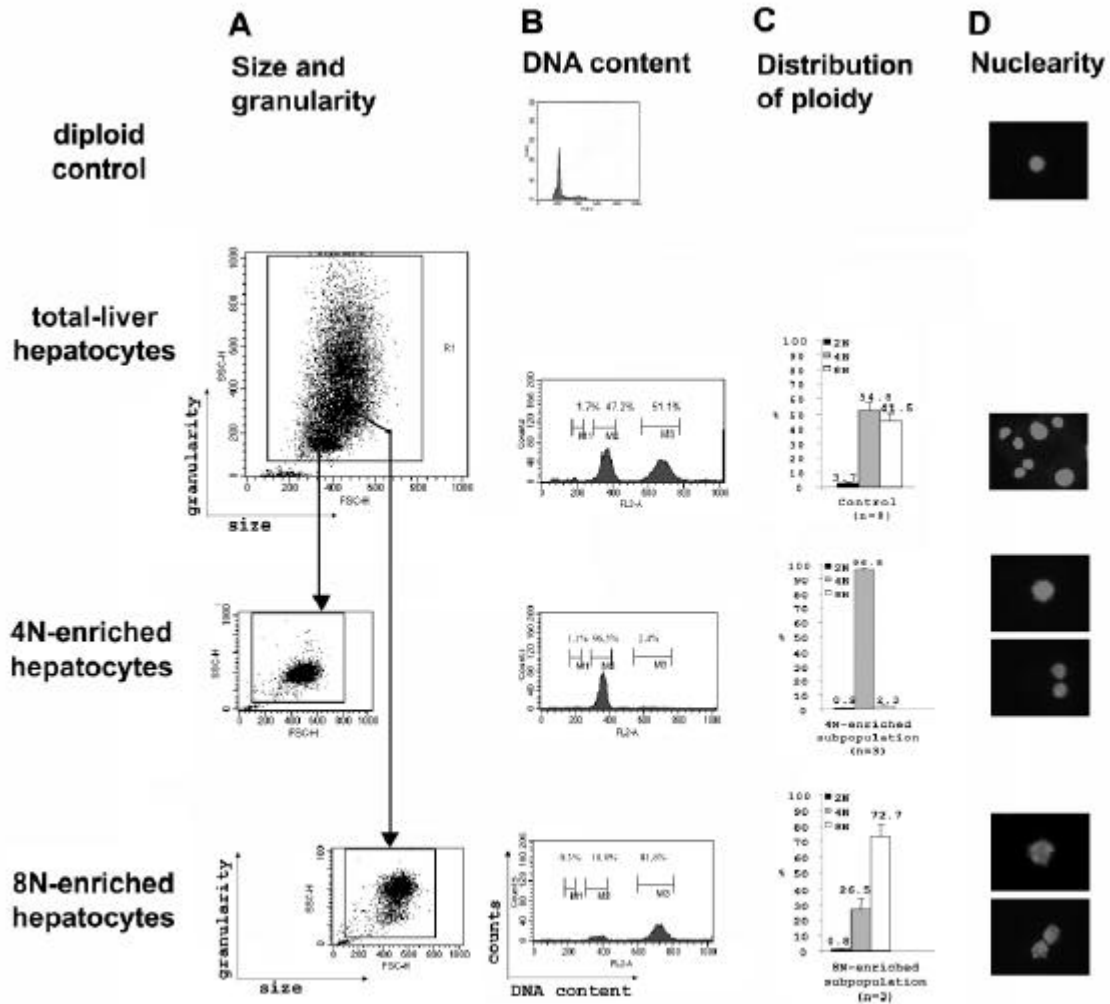


Figure 6

A

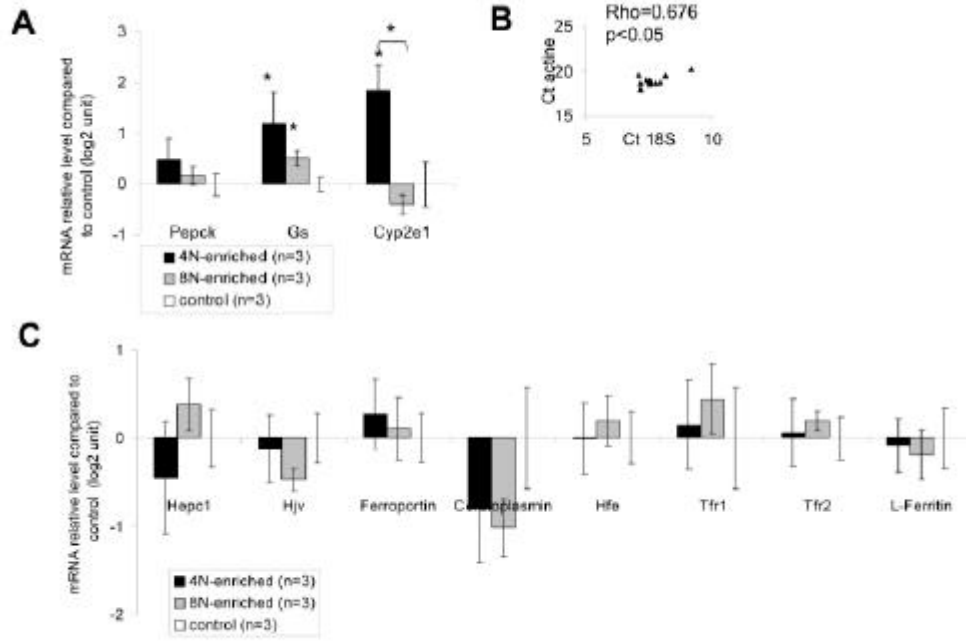


Figure 7